Analysis and design of reduced order linear quadratic regulator control for three phase power factor correction using Cuk rectifiers

M.G. Umamaheswari [a,b,*], G. Uma [a]

[a] Department of Electrical and Electronics Engineering, College of Engineering, Anna University, Chennai 600 025, Tamil Nadu, India
[b] Department of Electronics and Instrumentation Engineering, R.M.K. Engineering College, Kavaraipettai 601 206, Tamil Nadu, India

ABSTRACT

In this paper, the analysis and design of reduced order linear quadratic regulator (ROLQR) control for power factor correction (PFC) in a three phase system is presented. The front end is a three phase diode rectifier followed by DC–DC Cuk converter modules with the common DC output. Instantaneous symmetrical component theory is used for the generation of reference current. The control strategy uses three inner ROLQR current controllers for source current shaping and an outer voltage loop using PI controller for load voltage regulation. It uses a single stage converter for both PFC and voltage regulation. The proposed method offers simple control strategy, fast transient response and power factor closed to unity. This type of three-phase three switch PFC converter features a simple and robust configuration compared to conventional six switch topology. To validate the proposed method, a prototype controlled by dSPACE 1104 signal processor is set up. Simulation and experimental results indicate that the proposed system offers regulated output voltage for wide load variations and power factor close to unity.

© 2012 Elsevier B.V. All rights reserved.

1. Introduction

Recently, there is growing awareness about line pollution and deteriorating power factor due to the usage of pervading inductive and non-linear loads. Although many solutions were offered for single phase power factor correction (PFC), three phase active PFC was seldom considered. As all high power equipment derive electrical power from three phase mains, incorporating an active three phase PFC front end can contribute significantly in improving the overall power factor and reducing line pollution. Many literature have been proposed for PFC. A three-phase single switch PFC topology has the merits of simple control and few components [1–5]. This type of converter suffers due to Discontinuous Conduction Mode (DCM) operation, causing high current stresses on the power devices. A three phase six switch Pulse Width Modulation (PWM) boost rectifier is widely used for high-power applications. Advantages of this type of rectifier are high efficiency and good current quality. But the PWM rectifier needs a complex control structure and the efficiency is lower than the diode rectifier due to additional switching losses [6–13]. A three-phase three-switch topology composed of three single-phase single-switch modules was proposed for PFC in [14,15]. Even though the above method offers simple control implementation, it fails to operate in case of one or two module failures. A derived version of buck boost rectifier is a Cuk rectifier that inverts the voltage polarity and can also simultaneously increase or decrease the voltage magnitude. It has excellent features such as capacitive energy transfer, magnetic components integrability, full transformer utilization and good steady-state performance. It also provides smooth input and output currents due to the presence of inductors in the input and output side [16].

Many methods for generating the reference template were proposed. In [17–19] the instantaneous reactive power theory was proposed (i.e. p–q theory) for calculating the reference currents. The general equation for deriving the reference current which relates the new concept of instantaneous active and reactive theory was reported in [20], but no detailed information was given for DC bus voltage compensation. In [21], the extended p–q theory was proposed to derive a more general vector equation for calculating the reference currents. This method does not operate satisfactorily for module loss. In [22], only the final formulation of the extracted reference current was reported. In [23] and [24], PFC using Cuk rectifier modules was proposed and reference current was generated using power balance control technique. The extraction of reference current based on instantaneous symmetrical component theory involves simple computations based on the instantaneous

* Corresponding author at: Department of Electrical and Electronics Engineering, College of Engineering, Anna University, Chennai 600 025, Tamil Nadu, India. Tel.: +91 8148747320.
E-mail addresses: umagopinathh@gmail.com (M.G. Umamaheswari), uma@annauniv.edu (G. Uma).

source voltages and currents and it does not require any three phase to two phase conversions.

The classic Linear Quadratic Regulator (LQR) approach deals with the optimization of a cost function or performance index. Thus, the designer can weigh which states are more important in the control action to seek for appropriate performance. This feature of LQR control has initiated several researchers to successfully apply this technique in the field of power electronics. In [25] and [26], the performance indices are selected using pole placement technique. This method depends on the exact placement of closed loop poles. In [27], the cost function is derived from an initial controller by frequency domain method which is a time consuming procedure. Optimal control provides a systematic way of designing a LQR controller and problem of where to place the closed loop poles does not arise and is robust to parameter and load variations.

Hence, it is proposed to develop a single stage three phase AC–DC converter using Cuk rectifier modules based on ROLQR control for achieving voltage regulation and PFC. The instantaneous symmetrical component theory is used for calculating the reference currents. To reduce the complexity in analysis, a reduced order model of Cuk converter is obtained from the higher order state space model [28,29] by Pade's approximation technique. The outer voltage loop compensator is designed using Ziegler Nichol's tuning procedure.

2. Modeling of DC–DC Cuk converter

Fig. 1(a) represents the circuit diagram of the Cuk converter. It consists of two inductors L_i, L_o and two capacitors C_t, C_o, V_g and V_o represent supply and output voltage, respectively, S is an active switch, D is a freewheeling diode and R_L is the load resistance. S operates at a switching frequency f_s with duty ratio d.

To obtain the mathematical model of the controller, the state model of Cuk converter is derived by considering $S = 1$ during the MOSFET switch conduction subinterval and $S = 0$ during the diode conduction subinterval. The converter dynamics is described by state–space averaging method and by using the same method, the state equations during switch-on and switch-off conditions are combined as follows:

$$\frac{dx_1}{dt} = -\frac{(1-d)}{L_i}x_3 + \frac{V_g}{L_i} \tag{1}$$

$$\frac{dx_2}{dt} = \frac{d}{L_o}x_3 - \frac{1}{L_o}x_4 \tag{2}$$

$$\frac{dx_3}{dt} = \frac{(1-d)}{C_t}x_1 - \frac{d}{C_t}x_2 \tag{3}$$

$$\frac{dx_4}{dt} = \frac{1}{C_o}x_2 - \frac{1}{R_L C_0}x_4 \tag{4}$$

where x_1, x_2, x_3, x_4 are the current through the inductor (i_{Li}), current through the inductor (i_{Lo}), voltage across the transfer capacitor (v_{ct}), voltage across the output capacitor (v_{co}), respectively, and d represents the duty cycle. From Eqs. (1)–(4), the averaged system matrices are derived as given below:

$$A = \begin{bmatrix} 0 & 0 & \frac{-(1-d)}{L_i} & 0 \\ 0 & 0 & \frac{d}{L_o} & -\frac{1}{L_o} \\ \frac{(1-d)}{C_t} & -\frac{d}{C_t} & 0 & 0 \\ 0 & \frac{1}{C_o} & 0 & -\frac{1}{R_L C_o} \end{bmatrix}, \quad B = \begin{bmatrix} \frac{1}{L_i} \\ 0 \\ 0 \\ 0 \end{bmatrix} \tag{5}$$

2.1. Design of DC–DC Cuk converter components

A Cuk PFC was designed [23] with the following specifications: rectified input voltage $V_g = 24$ V, line frequency 50 Hz, power factor ≥ 0.99, maximum output power $P_o = 56$ W, $R_L = 10 \, \Omega$, output DC voltage $V_o = -24$ V, efficiency $\eta \geq 85\%$. DC voltage conversion ratio M is given by

$$M = \frac{V_o}{V_g} = 0.704 \tag{6}$$

Conduction parameter of the Cuk PFC circuit

$$K_a > \frac{1}{(2(M + |\sin(\theta)|)^2)} > 0.1752 \tag{7}$$

An equivalent inductance is given by

$$L_{eq} = \frac{R_L T_S K_a}{2} = 0.667 \text{ mH} \tag{8}$$

By choosing the input inductor current with 6.75% current ripple, $\Delta i_{Li} = 0.169$ A. The design of L_i and L_o is made using the desired ripple value of the input current. For the duty ratio $d = 0.5$, switching frequency = 50 kHz, switching period $T_s = 0.25 \, \mu$s, the input inductor value is found to be

$$L_i = \frac{V_g d T_S}{\Delta i_{Li}} = 2 \text{ mH} \tag{9}$$

The output inductor value is found to be

$$L_o = \frac{L_1 L_{eq}}{L_1 - L_{eq}} = 1 \text{ mH} \tag{10}$$

Transfer capacitor value is calculated by considering a resonant frequency of 1 kHz and is given by

$$C_t = \frac{1}{\omega_{ro}^2 (L_i - L_o)} = 25.35 \, \mu\text{F} \tag{11}$$

To select the output capacitance value in this circuit, the main factor is the output ripple voltage which is caused by the second harmonic. The equation to define the output capacitance value can be expressed as

$$C_o = \frac{P_{in}}{2\pi f_r V_o \Delta V_o} = 2211 \, \mu\text{F} \tag{12}$$

where ΔV_o is the peak value of the output ripple voltage = 0.6 V (2.5% of the output voltage) and f_r is the second harmonic frequency. The design values are substituted in (5) and after applying phase variable transformation, A and B matrices become,

$$A = \begin{bmatrix} 0 & 1 & 0 & 0 \\ 0 & 0 & 1 & 0 \\ 0 & 0 & 0 & 1 \\ -6.3 \times 10^{12} & -1.87 \times 10^9 & -3.8 \times 10^7 & -50 \end{bmatrix}, \quad B = \begin{bmatrix} 0 \\ 0 \\ 0 \\ 1 \end{bmatrix} \tag{13}$$

The main objective is to shape the input source current and to regulate the output voltage of the DC–DC Cuk converter. The converter requires sensing of four state variables, which is not acceptable from practical point of view. In order to reduce the complexity in controller design, the fourth order model of a Cuk converter is reduced to a second order model. The model reduction technique used is Pade's approximation, wherein the two dominant poles of the system i.e. the input inductor current, i_{Li} and the output capacitor voltage, v_{Co} are retained and the effects of the transfer capacitor C_t, and the output inductor L_o are neglected. Hence it becomes sufficient to regulate these two variables i_{Li}, v_{Co} using the ROLQR control strategy. The reduced order matrix for the above system is given as

$$A = \begin{bmatrix} 0 & 1 \\ -1.64 \times 10^5 & -49.34 \end{bmatrix}, \quad B = \begin{bmatrix} 0 \\ 1 \end{bmatrix} \tag{14}$$
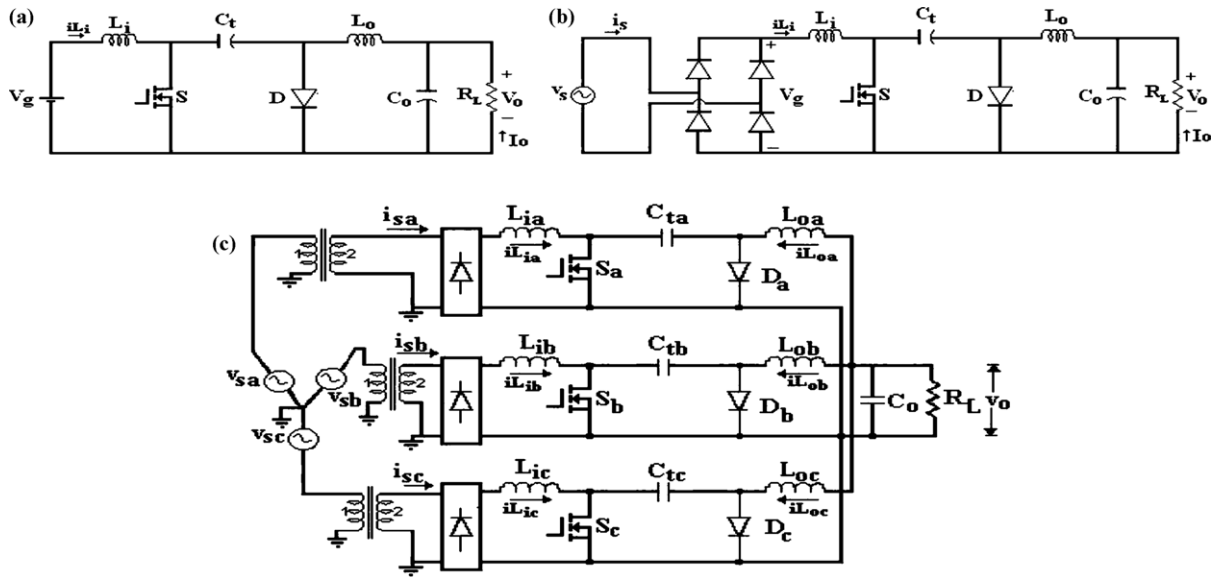
Fig. 1. (a) Circuit diagram of DC–DC Cuk converter. (b) Circuit diagram of single phase Cuk PFC rectifier. (c) Circuit diagram of the three phase Cuk PFC rectifier module.

2.2. Cuk rectifier module

The circuit diagram of the single phase Cuk PFC is shown in Fig. 1(b). The converter is designed using the design values outlined in the previous section. The circuit diagram of the proposed three phase configuration using single phase topology is shown in Fig. 1(c). L_{ia}, L_{ib}, L_{ic} represent the input inductors and L_{oa}, L_{ob}, L_{oc} represent the output inductors for the respective three phases a, b, c respectively. C_{ta}, C_{tb}, C_{tc} represent the transfer capacitors. v_{sa}, v_{sb}, v_{sc} and v_o represent supply voltages for the three phases and output voltage, respectively, S_a, S_b, S_c are active switches for the three phases, D_a, D_b, D_c are freewheeling diodes and R_L is the load resistance. All power devices of the PFC circuit, including the diode rectifier and the power circuit components of the Cuk converter are modularized. A single capacitor C_o is connected at the output terminals for filtering the output voltage ripple.

2.3. Generation of reference currents

The theory of instantaneous symmetrical components can compensate any kind of harmonics under balanced supply conditions. Reference current generation based on symmetrical component theory is explained in Fig. 2. Based on this theory, the reference current for the three phase balanced supply is given by

$$i_{sa} = \frac{v_{sa} + (v_{sb} - v_{sc})\beta*}{\left(v_{sa}^2 + v_{sb}^2 + v_{sc}^2\right)}(P_{Load} + P_{Loss}) \tag{15}$$
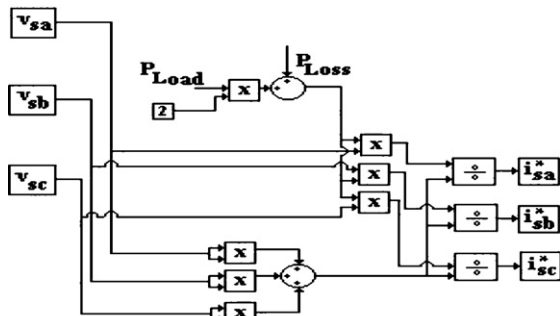

Fig. 2. Implementation of Instantaneous Symmetrical Component Theory.

$$i_{sb} = \frac{v_{sb} + (v_{sc} - v_{sa})\beta*}{\left(v_{sa}^2 + v_{sb}^2 + v_{sc}^2\right)}(P_{Load} + P_{Loss}) \tag{16}$$

$$i_{sc} = \frac{v_{sc} + (v_{sa} - v_{sb})\beta*}{\left(v_{sa}^2 + v_{sb}^2 + v_{sc}^2\right)}(P_{Load} + P_{Loss}) \tag{17}$$

where $e = V_{ref} - V_o$ and $\beta* = \tan \varphi / \sqrt{3}$, φ is the desired phase angle between supply voltages (v_{sa}, v_{sb}, v_{sc}) and source line currents (i_{sa}, i_{sb}, i_{sc}) for the balanced system. Here φ is taken as zero and P_{Local} is the load power and is given by

$$P_{Load} = V_o \times I_{Load} \tag{18}$$

Here the term P_{Loss} represents the switching losses and ohmic losses in the converter. Due to losses in converter, the capacitor voltage will decrease. When the capacitor voltage falls below the reference voltage; the PFC rectifier may not be able to track the reference current faithfully. So a suitable PI controller is used which regulate the voltage of capacitor to the reference value. P_{Loss} is thus given by

$$P_{Loss} = K_p e + K_i \int e \, dt \tag{19}$$

3. Control scheme

This section presents the design of the controller. The controller is comprised of three inner ROLQR current controllers for shaping the source current and an outer voltage control loop using PI controller to regulate the output voltage as shown in Fig. 3.

3.1. Principle of PI controller

A Proportional Integral (PI) compensator is selected for providing DC voltage regulation. The output voltage V_o is sensed and compared with reference voltage V_{ref} and the error is processed by the PI controller to keep the output voltage constant. The values of K_p and K_i are found by Ziegler–Nichols tuning method. The tuning method provides sustained oscillations with the ultimate gain $K_u = 4$ and ultimate period $P_u = 0.065$ s. By this technique, the exact values for $K_p(=K_u/2)$ and K_i are found to be 2 and 18.46 ($T_i = P_u/1.2$, $K_i = 1/T_i$), respectively. The closed loop operation of proposed
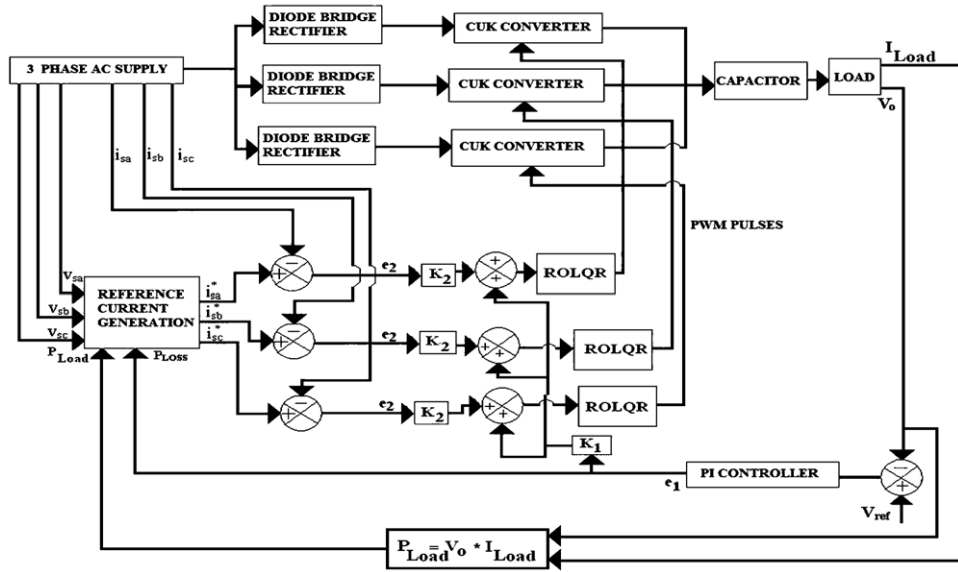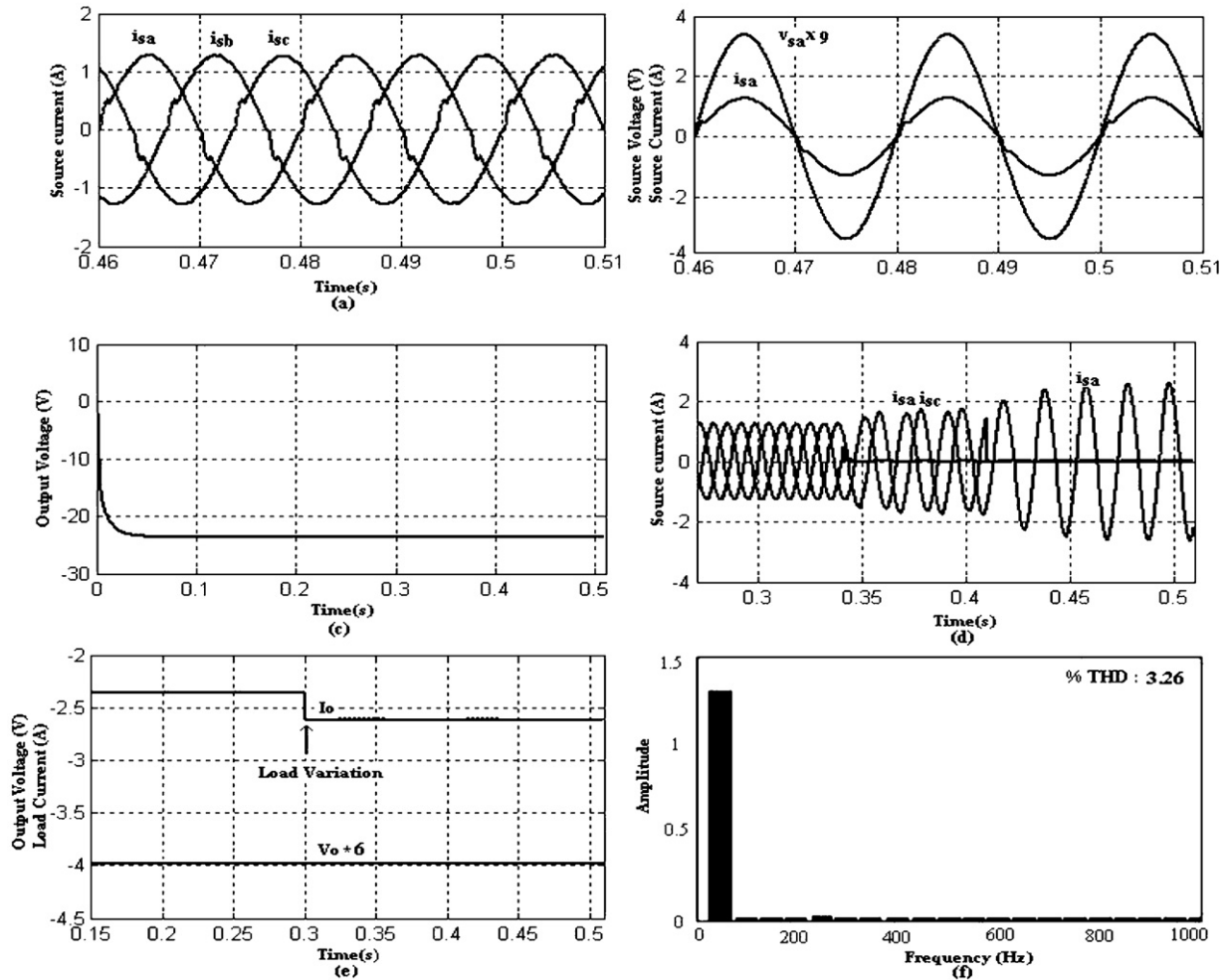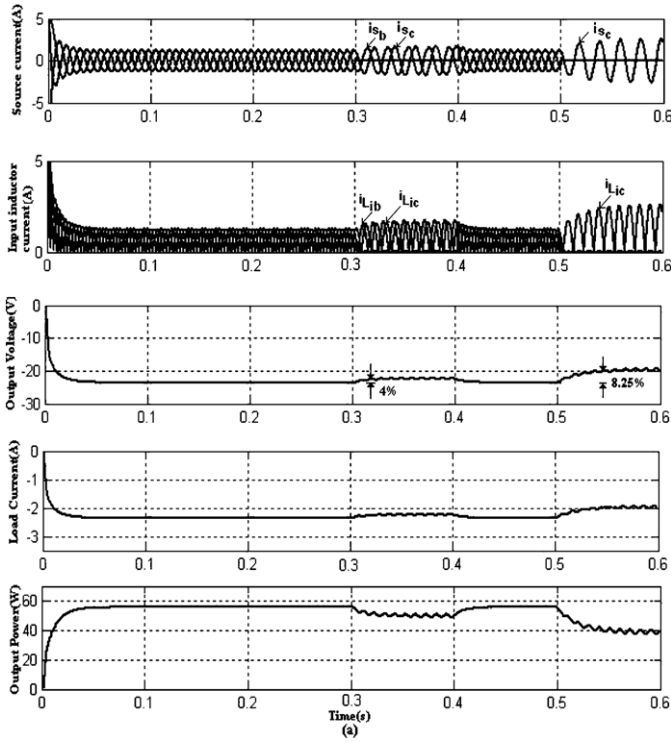
Fig. 3. Implementation of ROLQR control.

Fig. 4. Simulated waveforms for ROLQR control (a). Three phase source currents (b). UPF operation in phase-a (c). Regulated output voltage (d). Source currents with module loss (e). Regulated voltage and load current for step change in load (f). Spectrum of source current in phase-a.

Fig. 5. Simulation results for the source currents, inductor currents, output voltage and load current and output power for symmetric mains condition, module loss in phase a, module loss in phases a and b for ROLQR control.

system using outer PI controller and inner ROLQR controller is depicted in Fig. 3.

3.2. Reduced order linear quadratic regulator control

The theory of optimal control is concerned with operating a dynamic system at minimum cost. The time invarying linear quadratic regulator is used as tracking current controller. Here for the proposed system ROLQR gain matrix is computed by appropriately choosing values of R and Q (weight matrix). The values for Q and R matrices are

$$Q = \begin{bmatrix} 1.16 \times 10^7 & 0 \\ 0 & 1 \end{bmatrix}, \quad R = [1] \tag{20}$$

Q matrix is chosen in such a way that maximum weightage is given to input inductor current, so that input current shaping is performed more effectively by ROLQR controller. Q and R should be positive semi-definite and positive definite, respectively. They are selected such that the scalar quantity $x^T Q x$ is always positive or zero at each time t for all functions $x(t)$, and the scalar quantity $u^T R u$ is always positive at each time t for all values of $u(t)$. In terms of eigen values, the eigen values of Q should be non-negative, while those of R should be positive.

For a continuous time system, the state-feedback control law $u = -K_F x$ minimizes the quadratic cost function

$$J(x(\cdot), u(\cdot)) = \frac{1}{2} \int_{t_0}^{t_f} (x^T Q x + u^T R u) dt \tag{21}$$

Subject to the system dynamics

$$X^\bullet = AX + BU \tag{22}$$

For the proposed system, the quadratic cost function is obtained after substituting the values of X, Q, R in Eq. (21)

$$\int_{t_0}^{t_f} [(1.16 \times 10^7 x_1^2 + x_2^2) + u^2] dt \tag{23}$$

The control law is found to be

$$u = -R^{-1} B^T K x = u = -K_F x \tag{24}$$

where K_F is the feedback gain matrix and K is the return function matrix. The unknown coefficients of the return function matrix are found by solving the Ricatti equation

$$-Q - A^T K - KA + KBR^{-1}B^T K = 0 \tag{25}$$

$$
-\begin{bmatrix} 1.16 \times 10^7 & 0 \\ 0 & 1 \end{bmatrix} - \begin{bmatrix} 0 & -1.64 \times 10^5 \\ 1 & -49.34 \end{bmatrix} \begin{bmatrix} k_{11} & k_{12} \\ k_{21} & k_{22} \end{bmatrix}
$$
$$
-\begin{bmatrix} k_{11} & k_{12} \\ k_{21} & k_{22} \end{bmatrix} \begin{bmatrix} 0 & 1 \\ -1.64 \times 10^5 & -49.3 \end{bmatrix} +
$$
$$
\begin{bmatrix} k_{11} & k_{12} \\ k_{21} & k_{22} \end{bmatrix} \begin{bmatrix} 0 \\ 1 \end{bmatrix} [1] \begin{bmatrix} 1 & 0 \end{bmatrix} \begin{bmatrix} k_{11} & k_{12} \\ k_{21} & k_{22} \end{bmatrix} = 0 \tag{26}
$$

On solving Eq. (26), the return function matrix K is found to be

$$\begin{bmatrix} k_{11} & k_1 \\ k_{21} & k_{22} \end{bmatrix} = \begin{bmatrix} 1.2 \times 10^5 & 40 \\ 40 & 1 \end{bmatrix} \tag{27}$$

On substituting the value of K matrix in the equation, $K_F = -R^{-1}B^T K$ the feed back gain matrix K_F is obtained. It is found to be $\begin{bmatrix} 35.362 & 0.7216 \end{bmatrix}$.

Hence the control law becomes

$$u = -35.362(x_{1\text{ref}} - x_1) - 0.7216(x_{2\text{ref}} - x_2) \tag{28}$$

Eq. (28) is rewritten as

$$u = -(K_1 e_1 + K_2 e_2) \quad \text{where} \quad K_1 = 35.362 \text{ and } K_2 = 0.7216 \tag{29}$$

3.2.1. Closed loop control using ROLQR

The proposed ROLQR scheme is illustrated in Fig. 3, where PI controller and ROLQR act as outer voltage controller and inner current controllers, respectively. The output voltage is compared with the reference voltage and the error e_1 is fed to the PI controller. Reference currents are generated using the output of the PI controller, i.e. P_{Loss}, three phase source voltages v_{sa}, v_{sb}, v_{sc} and the load power P_{Load}. The reference currents with desired magnitude and shape are derived by instantaneous symmetrical component theory. The instantaneous values of actual current and reference current are compared and the error is found to be e_2. The inputs to the ROLQR are voltage error e_1 and the current error e_2 for each phase. The output u is the control signal in each phase, which in turn sets the new duty ratio of the switching pulses for triggering the switches S_a, S_b, S_c.

4. Simulation studies

A simulation model of the three phase AC–DC converter formed by single phase Cuk rectifier modules controlled using PI controller for output voltage regulation and ROLQR for UPF operation is developed in MATLAB/SIMULINK. The entire system is simulated. The simulation results of the proposed scheme using ROLQR are shown in Fig. 4(a)–(e). It can be seen from Fig. 4(a) and (b) that almost unity power factor and nearly sinusoidal current operation is achieved. It is understood from Fig. 4(c) that the proposed system also provides regulated output voltage. Fig. 4(d) shows the source currents under
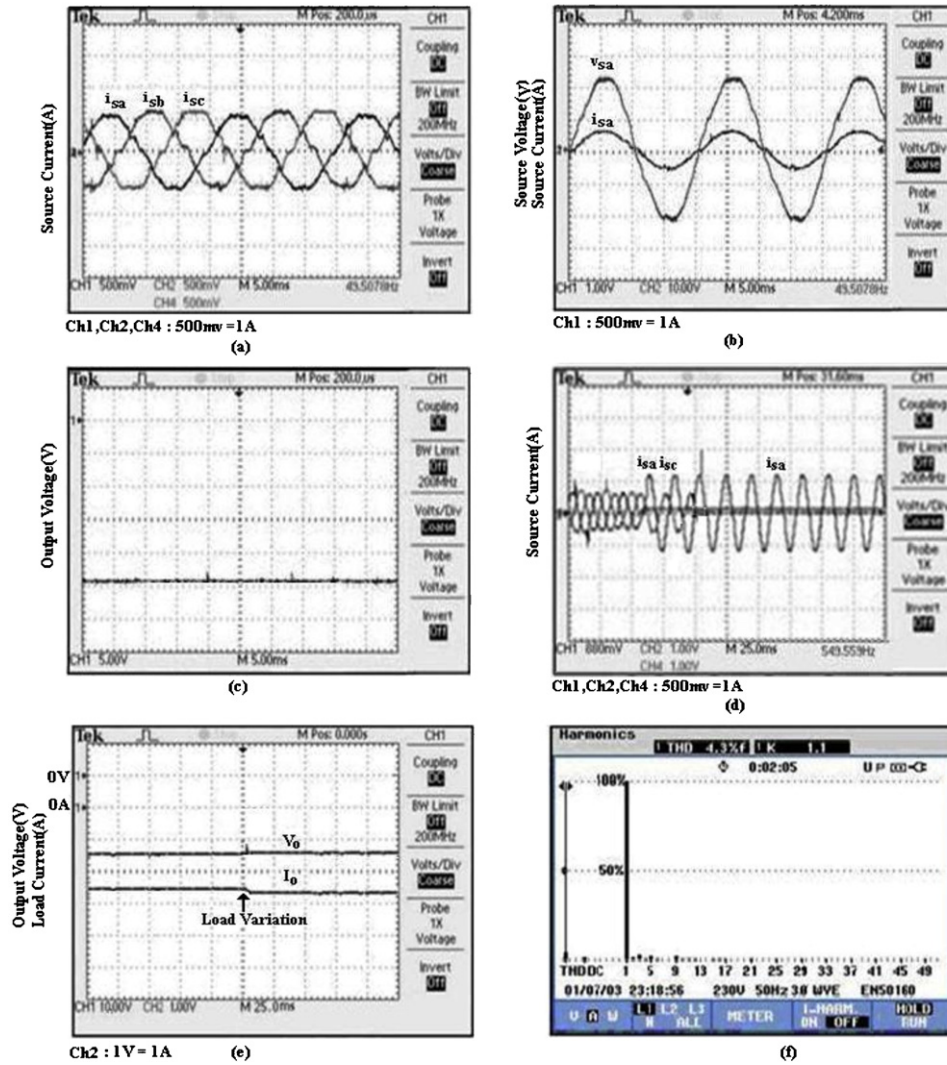
Fig. 6. Experimental waveforms for ROLQR control (a). Three phase source currents (b). UPF operation in phase-a (c). Regulated output voltage (d). Source currents with module loss (e). Regulated voltage for step change in load (f). Spectrum of source current in phase-a.

module loss conditions. All the three-phase supply condition exists between 0.29 and 0.34 s and module loss occurs in phase b between 0.34 and 0.41 s: and module loss occurs in phases b and c between 0.41 and 0.51 s. The simulation result of transient response of the output voltage and load current waveforms for step load change is shown in Fig. 4(e) and it is observed that the output voltage is maintained constant for a step load change. Here, each single phase PFC Cuk module is designed for the rated load current. In the three phase configuration, each Cuk module carries one-third of load current. Hence, from Fig. 4(d), it is observed that, even under single/two module loss conditions, the system continues to work and maintain the output voltage nearer to the desired value. Under one module loss conditions, the magnitude of the source currents are unequal and it is due to the presence of an oscillating component in the power PLavg. From Fig. 4(f), the %THD is found to be 3.26. Fig. 5 shows the simulation results of the input line currents,

inductor currents, output voltage, load current and output power for symmetric mains condition, module loss in phase a, module loss in phases a and b.

5. Experimental studies

A prototype is constructed in order to experimentally test the ROLQR control method using the following specifications $f_s = 50$ kHz, $V_s = 24\,V_{rms}$, $L_{ia}, L_{ib}, L_{ic} = 2$ mH, $L_{oa}, L_{ob}, L_{oc} = 1$ mH, $C_{ta}, C_{tb}, C_{tc} = 25\,\mu$F, $C_o = 2000\,\mu$F, $R_L = 10\,\Omega$ using dSPACE 1104 signal processor. The input and output inductors are of ferrite core type and the capacitors are of plain polyester type. Power MOSFET IRF540N is used as a switch and IN 4007 is used as a diode. The 12 bit ADC unit in the dSPACE accepts a maximum analog input voltage of ±10 V. During the closed loop operation the three phase source voltages and source currents, output voltage and current are sensed by hall

Table 1
A summary of system performance parameters for the variation of load.

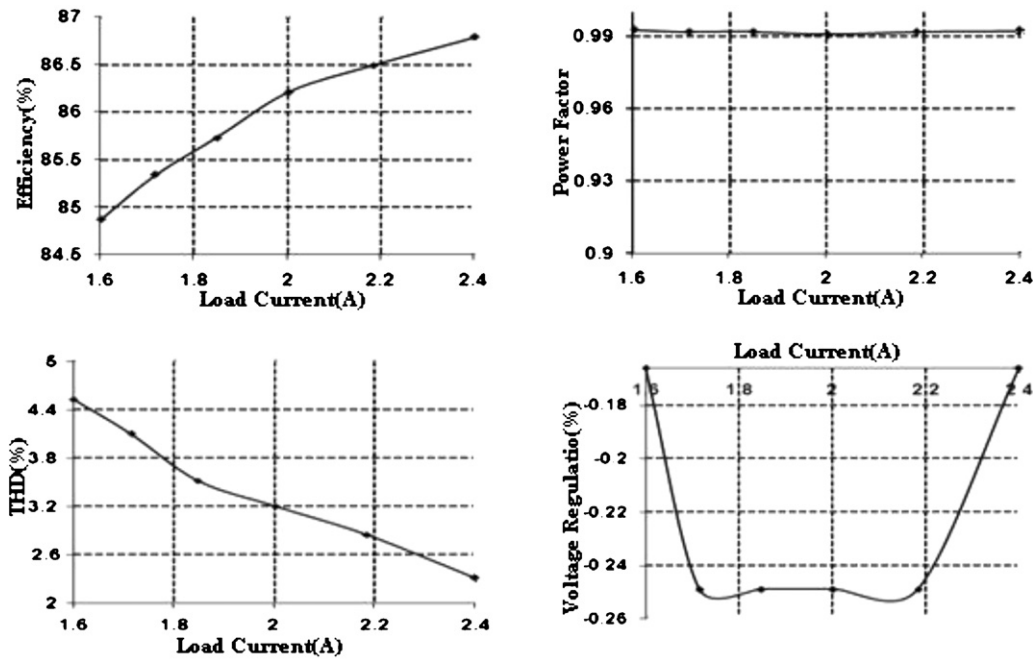| Load current (A)	2.404	2.186	2.004	1.85	1.718	1.603
Efficiency (%)	86.79	86.49	86.21	85.73	85.34	84.88
PF	0.9921	0.9919	0.9919	0.9919	0.9918	0.9916
THD	2.311	2.847	3.203	3.521	4.102	4.532
Voltage regulation (%)	−0.166	−0.249	−0.249	−0.249	−0.249	−0.166

Fig. 7. Graphical representation of data given in Table 1 illustrates the system performance as the load is varied.

effect voltage and current sensors and scaled down to less than ± 10 V using the signal conditioning circuit.

The ADC signals are processed by the proposed ROLQR algorithm to calculate the new duty ratio for the switches S_a, S_b, S_c. The PWM pulses obtained from dSPACE unit is used to trigger the MOSFET switches S_a, S_b, S_c using IR2110 driver. Fig. 6 depicts the experimental results of the proposed converter module. Fig. 6(a) reveals that source current becomes sinusoidal after implementing ROLQR control. UPF operation at the line side under constant load conditions, tight regulation of the DC output voltage is evident from Fig. 6(b) and (c). Fig. 6(d) shows the source currents under module loss conditions. Fig. 6(e) shows that the converter gets back its reference voltage for step change in load. The closed loop control of Cuk rectifier module using ROLQR forces the source current to follow the source voltage more effectively and it is also proved by viewing the harmonic spectrum of source current which is shown in Fig. 6(f) and the %THD is found to be 4.3%. Table 1 presents the variation of performance parameters as a function of load current and the performance curves are depicted in Fig. 7.From Fig. 7, it is observed that the % efficiency is maintained around 85% for all the loads and the maximum efficiency at rated load is found to be 86.79% at nominal load current of 2.404 A. The %THD is almost maintained constant and the power factor is also maintained around unity irrespective of the load variation which shows the effectiveness of ROLQR control.

6. Discussion

It is proposed to construct a ROLQR based single stage Cuk converter in modular form for achieving PFC and voltage regulation. All the control circuits including the PI controller, reference current generation using instantaneous symmetrical component theory and inner ROLQR control loop have been implemented using dSPACE signal processor. There is a difference in %THD between simulation and experimentation, because the internal resistances of reactive elements, semiconductors that may slightly influence the dynamic of the converter, which is not appearing when simulated with ideal components. Moreover the power quality analyzer used in experimentation is able to trap only up to 49th harmonic.

7. Conclusion

In this paper, the analysis and design of a single stage three phase AC to DC converter formed by DC Cuk rectifier modules with the common DC output for PFC was presented. Reference current was generated using instantaneous symmetrical component theory .The control strategy is based on outer voltage control loop and three inner ROLQR current controllers. To support the proposed method, a prototype controlled by dSPACE signal processor was set up. The variation of performance parameters of Cuk rectifier modules with the load variation proves the robustness and effectiveness of ROLQR control. Simulation and experimental results reveal that the proposed system offers the regulated output voltage for step load variations and also provide power factor close to unity.

References

[1] H.-J. Chiu, T.-H. Wang, L.-W. Lin, Y.-K. Lo, Current imbalance elimination for a three-phase three-switch PFC converter, IEEE Transactions on Power Electronics 23 (March (2)) (2008) 1020–1022.
[2] R.L. Alves, I. Barbi, Analysis and implementation of a hybrid high-power-factor three-phase unidirectional rectifier, IEEE Transactions on Power Electronics 24 (March (3)) (2009) 632–640.
[3] G. Spiazzi, F.C. Lee, Implementation of single-phase boost power-factor-correction circuits in three-phase applications, IEEE Transactions on Industrial Electronics 44 (June (3)) (1997) 365–371.
[4] A.R. Prasad, P.D. Ziogas, S. Manias, An active power factor correction technique for three-phase diode rectifiers, IEEE Transactions on Power Electronics 6 (January (1)) (1991) 83–92.
[5] L. Dalessandro, S.D. Round, J.W. Kolar, Center-point voltage balancing of hysteresis current controlled three-level PWM rectifiers, IEEE Transactions on Power Electronics 23 (September (5)) (2008) 2477–2488.
[6] C. Qiao, K.M. Smedley, Unified constant-frequency integration control of three-phase standard bridge boost rectifiers with power-factor correction, IEEE Transactions on Industrial Electronics 50 (February (1)) (2003) 100–107.
[7] S. Chattopadhyay, V. Ramanarayanan, Digital implementation of a line current shaping algorithm for three phase high power factor boost rectifier with out input voltage sensing, IEEE Transactions on Power Electronics 19 (May (3)) (2004) 709–721.
[8] S. Chattopadhyay, V. Ramanarayanan, A voltage-sensorless control method to balance the input currents of a three-wire boost rectifier under unbalanced input voltages condition, IEEE Transactions on Industrial Electronics 52 (2) (2005) 386–398.
[9] R. Ghosh, G. Narayanan, Control of three-phase, four-wire PWM rectifier, IEEE Transactions on Power Electronics 23 (January (1)) (2008) 96–106.

[10] X.H. Wu, S.K. Panda, J.X. Xu, DC link voltage and supply-side current harmonics minimization of three phase PWM boost rectifiers using frequency domain based repetitive current controllers, IEEE Transactions on Power Electronics 23 (July (4)) (2008) 1987–1997.

[11] P. Xiao, K.A. Corzine, G.K. Venayagamoorthy, Multiple reference frame-based control of three-phase PWM boost rectifiers under unbalanced and distorted input conditions, IEEE Transactions on Power Electronics 23 (July (4)) (2008) 2006–2017.

[12] A.H. Bhat, P. Agarwal, Three-phase, power quality improvement ac/dc converters, Electric Power Systems Research (2007) 276–289.

[13] Y. Neba, K. Ishizaka, R. Itoh, Single-phase two-stage boost rectifiers with sinusoidal input current, IET Power Electronics 3 (March (2)) (2010) 176–186.

[14] Y.K. Eric Ho, S.Y.R. Hui, Y.-S. Lee, Characterization of single-stage three-phase power-factor-correction circuit using modular single-phase PWM DC-to-DC converters, IEEE Transactions on Power Electronics 15 (January (1)) (2000) 62–71.

[15] S. Kim, P.N. Enjeti, A modular single-phase power-factor-correction scheme with a harmonic filtering function, IEEE Transactions on Industrial Electronics 50 (April (2)) (2003) 328–335.

[16] M.G. Umamaheswari, G. Uma, K.M. Vijayalakshmi, Design and implementation of reduced-order sliding mode controller for higher order power factor correction converters, IET Power Electronics 4 (November (9)) (2011) 984–992.

[17] H. Akagi, Y. Kanazawa, A. Nabae, Instantaneous reactive power compensators comprising switching device without energy storage components, IEEE Transactions on Industry Applications IA-20 (May/June (3)) (1984) 625–630.

[18] F.Z. Peng, J.-S. Lai, Generalized instantaneous reactive power theory for three-phase power systems, IEEE Transactions on Instrumentation and Measurement 45 (February (1)) (1996) 293–297.

[19] S.J. Huang, J. Chang-Wu, A new control algorithm for three phase three wire active filters under non ideal main voltages, IEEE Transactions on Power Electronics 14 (July (4)) (1999) 3089–3094.

[20] M. Aredes, E.H. Watanabe, New control algorithms for series and shunt three phase four wire active filter, IEEE Transactions on Power Delivery 10 (July (3)) (1995) 1649–1656.

[21] M.K. Mishra, A. Joshi, A. Ghosh, A new compensation algorithm for balanced and unbalanced distribution systems using generalized instantaneous reactive power theory, Electric Power Systems Research 60 (2001) 29–37.

[22] C.C. Chen, Y.Y. Hsu, A novel approach to the design of a shunt active filter for unbalanced three phase four wire systems under non sinusoidal conditions, IEEE Transactions on Power Delivery 15 (October (4)) (2000) 1258–1264.

[23] U. Kamnarn, V. Chunkag, Analysis and design of a modular three phase AC-to-DC converter using CUK rectifier module with nearly unity power factor and fast dynamic response, IEEE Transactions on Power Electronics 24 (August (8)) (2009) 2000–2012.

[24] V. Chunkag, U. Kamnarn, Paralleling three-phase AC to DC converter using CUK rectifier modules based on power balance control technique, IET Power Electronics 3 (July (4)) (2010) 511–524.

[25] F.H.F. Leung, P.K.S. Tam, C.K. Li, An improved LQR-based controller for switching DC–DC converters, IEEE Transactions on Industrial Electronics 40 (October (5)) (1993) 521–528.

[26] F.H.F. Leung, P.K.S. Tam, C.K. Li, The control of switching DC–DC converters – A general LQR problem, IEEE Transactions on Industrial Electronics 38 (February (1)) (1991) 65–71.

[27] C. Gezgin, B.S. Heck, R.M. Bass, Control structure optimization of a boost converter: an LQR approach, in: Proceedings of IEEE PESC, vol. 2, 1997, pp. 901–907.

[28] S. Ang, et al., Power Switching Converter, Taylor and Francis Group, 2005.

[29] J.S. Bay, Fundamentals of Linear State Space Systems, McGraw-Hill Publishers, 1998.